Journal of Drug Delivery Science and Technology 43 (2018) 19–26

Contents lists available at ScienceDirect

Journal of Drug Delivery Science and Technology

journal homepage: www.elsevier.com/locate/jddst

The inhibitory effects of nano-encapsulated metformin on growth and hTERT expression in breast cancer cells

Shahrzad Javidfar [a, b], Younes Pilehvar-Soltanahmadi [b, c], Raana Farajzadeh [b], Javid Lotfi-Attari [b], Vahid Shafiei-Irannejad [c], Mehrdad Hashemi [a], Nosratollah Zarghami [b, c, *]

[a] Department of Genetics, Tehran Medical Sciences Branch, Islamic Azad University, Tehran, Iran
[b] Department of Medical Biotechnology, Faculty of Advanced Medical Sciences, Tabriz University of Medical Sciences, Tabriz, Iran
[c] Hematology and Oncology Research Center, Tabriz University of Medical Sciences, Tabriz, Iran

ARTICLE INFO

Article history:
Received 6 June 2017
Received in revised form
4 September 2017
Accepted 16 September 2017
Available online 18 September 2017

Keywords:
Metformin
PLGA-PEG
Nanoparticles
hTERT
Breast cancer

ABSTRACT

Metformin has recently received attention for its potential effects with respect to cancer prevention and treatment. Nonetheless, the low bioavailability and short half-life of metformin hamper its application as an anti-cancer drug. The present study aims to evaluate the efficiency of PLGA-PEG as a nanocarrier for metformin to enhance anticancer effects. For this purpose, metformin-loaded PLGA-PEG NPs were synthetized and characterized using DLS, FE-SEM and FTIR. Then, the inhibitory effects of free and nano-encapsulated forms of metformin on growth and expression levels of hTERT in two breast cancer cell lines, T47D and MDA-MB-231, were evaluated using MTT and qPCR assays, respectively. Assessment of drug toxicity revealed that metformin-loaded NPs had more cytotoxic effects than free form in both cell lines at a dose- and time-dependent manner. The IC50s of free and nanoformulated metformin for MDA-MB-231 cells were lower than T47D cells, indicating the higher sensitivity of the triple-negative phenotype. Also, it was found that nanoformulated metformin than free metformin could further decline the expression levels of hTERT in both cell lines, especially MDA-MB-231 ($p < 0.05$). It is speculated that nano-encapsulation of metformin into polymeric NPs may be a promising and convenient approach to improve its efficiency in breast cancer therapy.

1. Introduction

Breast cancer is the most common cancer among women worldwide [1,2]. About 12% U.S. women will develop invasive breast cancer over the during her lifetime. In 2017, an estimated 252,710 new cases of invasive breast cancer are predictable to be identified in U.S. women, along with 63,410 new cases of non-invasive breast cancer [3,4].

Traditional cancer therapies including chemotherapy, radiation, and surgery are frequently defective in treating breast cancer, so developing novel strategies of treatment are essential [5].

Telomerase has been used as a desirable target for diagnosis and treatment of various types of cancers, since it continues tumor cells division preserving them to survive and avoid apoptosis [6]. Telomerase is an enzyme complex containing a catalytic subunit, telomerase reverse transcriptase (TERT), and a telomerase RNA component (TR) for adding TTAGGG repeats to the end of the chromosome to maintain the length of the telomere which can lead to genomic instability [5]. It has been revealed in 90% of breast carcinomas and in excess of 85% of human cancers, telomerase is active while in normal cells it is not active or detectable [7]. In cancer cells, induction of telomerase activity bypasses normal cellular senesce and donates them with limitless replicative potential which is one of the major features of all cancer cells. Suppression of telomerase activity in cancer cells may reactivate telomere shortening and could be hopeful action in cancer therapy [7].

Metformin (N′, N′-dimethyl biguanide) is an inexpensive, FDA approved and well-tolerated oral drug which has been frequently applied as the first-line therapy for diabetes mellitus type 2 (structure shown in Fig. 1) [8]. In recent years, numerous reports have presented evidence proposing a potential role for metformin

* Corresponding author. Department of Medical Biotechnology, Faculty of Advanced Medical Sciences, Tabriz University of Medical Sciences, Tabriz, Iran.
E-mail address: zarghami@tbzmed.ac.ir (N. Zarghami).

http://dx.doi.org/10.1016/j.jddst.2017.09.013
1773-2247/

in anti-cancer therapy [9,10]. The function of metformin in the inhibition of cancer is suggested to be related to both direct and indirect effects of the drug. The indirect influences are associated to the capability of metformin to hinder the transcription of main gluconeogenesis genes in the liver and arouse glucose uptake in muscle, therefore enhancing insulin sensitivity and decreasing blood glucose and reducing insulin levels. The direct influences of metformin are thought to be principally mediated by stimulation of AMP-activated protein kinase (AMPK), a serine/threonine protein kinase involved in controlling cellular energy metabolism, causing a decrease in the mammalian target of rapamycin (mTOR) signaling and protein synthesis in cancer cells. Metformin stimulates AMPK by hindering complex I of the mitochondrial respiratory chain, which causes impaired mitochondrial role and situations that efficiently mimic cellular energy stress [10,11].

Metformin is a hydrophilic molecule with a cationic charge at physiological pH and hence, it has partial passive diffusion through cell membranes. Due to its low permeability through the cell membranes and high aqueous solubility, metformin has a short absorption window in the gastrointestinal tract, therefore displays weak bioavailability [12]. Also, it needs repeated doses of administration to provoke remedial response. To overcome these limitations, different approaches can be applied [13]. Novel formulation approaches for metformin are being followed which can cause an enhancement in bioavailability, a decrease in dosing frequency, and/or a reduction in gastrointestinal adverse effects [14,15]. Nanoparticulate drug delivery systems have many benefits in relative to traditional dosage forms [13,16]. As drug carriers, polymeric nanoparticles (NPs) have plenty of advantages such as high carrier capacity, high drug stability, long shelf life, possibility of loading of both hydrophobic and hydrophilic therapeutic agents, and feasibility of various routes of administration [16–18].

The surface of polymeric NPs such as poly (lactide-*co*-glycolide) (PLGA) exhibits a hydrophobic surface which is rapidly recognized by plasmatic opsonin and cleared by cells of the mononuclear phagocyte system. The opsonization process is one of the most important biological hindrances to NP-based controlled drug delivery approaches. Coating of the surface of NPs with hydrophilic polymers such as polyethylene glycol (PEG) inhibits the absorption of opsonin factors through steric repulsion forces and thus, the NPs become “invisible” to mononuclear phagocyte system, enhancing their plasmatic circulation period and resulting in an improvement in bioavailability and half-life of drugs. Moreover, extensive plasmatic circulation periods enhance the possibility of the NPs reaching their target [16].

The purpose of the current work is to synthesize metformin-loaded PLGA-PEG NPs and assess their cytotoxic effects on two breast cancer cell lines, T47D (luminal A) and MDA-MB-231 (triple negative). Moreover, the inhibitory effects of metformin-loaded PLGA-PEG NPs on hTERT expression levels as a possible inhibition mechanism were studied.

2. Materials and methods

2.1. Materials

The human breast cancer cell lines, T47D and MDA-MB-231, were provided from Cell Bank of Pasteur Institute of Iran (code: C203). Fetal Bovine Serum (FBS) and RPMI1640 were purchased from Gibco, Invitrogen, UK. Penicillin G, Streptomycin, Sodium bicarbonate, Glucose, Metformin hydrochloride, D L-lactide, glycolide, stannous octoate [$Sn(Oct)_2$], PEG (molecular weight 4000), Dichloromethane (DCM), polyvinyl alcohol (PVA, MW 30,000–70,000 Da), dimethyl sulfoxide (DMSO), MTT [3(4, 5-dimethyl thiazol-2-yl) 2, 5-diphenyl-tetrazolium bromide] were purchased from Sigma-Aldrich (St Louis, Missouri, USA). Syber green real time PCR master mix kit was provided from Thermo Fisher (Waltham, Massachusetts, USA). D, L-lactide and glycolide were recrystallized with ethyl acetate. PEG was dehydrated for 12 h at 70 °C under vacuum and was used without further purification.

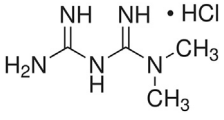

Fig. 1. Chemical structure of metformin hydrochloride.

2.2. Synthesis of PLGA-PEG copolymer

PLGA-PEG copolymers were synthesized through ring-opening polymerization method under vacuum based on previous studies [19,20]. According to the protocol, DL-lactide (2.882 g), PEG_{4000} (1.54 g) and glycolide (0.570 g) were melted in bottleneck flask in 140 °C under a N_2 atmosphere. Then 0.05% (w/w) $Sn(Oct)_2$ was added and the temperature was increased to 180 °C and maintained for 4 h. The copolymer was recovered by dissolving in DCM followed by precipitation in ice-cold diethyl ether.

2.3. Preparation of metformin-loaded PLGA-PEG NPs

PLGA-PEG NPs loaded with metformin were prepared via the double emulsion (w/o/w) method. Briefly, 200 mg of PLGA-PEG dissolved in 5 mL of DCM. The organic phase was added into 20 mL of PVA (0.5% w/v) containing metformin HCl 20 mg (the w/o primary mixture) and then emulsified using an ultrasonic probe (with 55% power) (Sonoplus, HD 2070; Bandelin Electronics, Berlin, Germany) for 2 min to produce w/o/w emulsion. Then, DCM was evaporated using a rotary evaporator (Heidolph Instruments, Hei-VAP series) at 40 °C and the remaining solution was collected by centrifugation at 15,000 rpm for 40 min min.

2.4. NPs characterizations

The NPs size (diameter, nm) was determined using a Dynamic Light Scattering (DLS) Zetasizer Nano ZS (Malvern Instruments Ltd., Malvern, UK) equipped with a helium–neon laser beam at a wavelength of 633 nm and a fixed scattering angle of 90. NPs were prepared by directly dissolving copolymers or drug-loaded NPs in deionized water at a concentration of 0.5 mg/mL followed using 10 min sonication at room temperature. Also, the size verification and surface morphology investigation of NPs were done using field emission scanning electron microscopy (FE-SEM) system (Hitachi S-4800 FE-SEM). NPs were coated with gold under vacuum before scanning electron microscopy.

A Perkin-Elmer Spectrum One model FT-IR was applied to record the IR spectra of free metformin, PLGA-PEG and metformin-Loaded PLGA-PEG NPs prepared in KBr disks in the region of 4000–400 cm^{-1}.

2.5. Drug encapsulation efficiency and drug loading

Following synthesis, the supernatant was collected and compared with the total amount of metformin to assess the metformin loading efficiency of the NPs. The amount of non-entrapped metformin in aqueous phase was determined at wavelengths 237 nm (λ-max) of metformin HCl using a Lambda 950 Visible-UV spectrophotometer (PerkineElmer Fremont, CA, USA). The percent

of metformin encapsulated on the NPs (EE) (Equation (1)) and drug loading (DL) (Equation (2)) were measured using the following formula:

$$EE = \frac{Weight\ of\ Metformin\ in\ NP}{Weight\ of\ the\ initial\ drug} \times 100\% \quad (1)$$

$$DL = \frac{Weight\ of\ Metformin\ in\ NP}{Weight\ of\ NPs} \times 100\% \quad (2)$$

In vitro drug release profile of metformin from drug loaded PLGA-PEG NPs were performed using the dialysis method as described previously [9]. Briefly, 20–30 mg of metformin-loaded NPs were dispersed in PBS (5 mL, pH = 4.4 or 7.4) and transmitted to dialysis membrane tubing (MW cut off: 3000) placed in 30 mL of PBS with stirring at 120 rpm at 37 °C. At selected time intervals, the environmental buffer solution was substituted with fresh PBS, and the concentration of the free metformin in the removed PBS was calculated applying a calibration curve at the wavelength where metformin displayed their maximum absorbance (237 nm), quantitatively examined using Lambda 950 Visible-UV spectrophotometer (PerkineElmer Fremont, CA, USA). Then, the accumulative ratios of the released metformin were determined as a function of time. All of the operations were performed in triplicate.

2.6. Cytotoxicity assay

The cytotoxicity of metformin-loaded PLGA-PEG NPs were evaluated using the MTT (3- [4, 5-dimethylthiazol-2yl]-2, 5-diphenyl tetrazolium bromide) assay. It is based on the capacity of mitochondrial succinate dehydrogenase in living cells to decrease the yellow water-soluble tetrazolium salt into an insoluble, colored formazan complex which is measured spectrophotometrically. First, T47D and MDA-MB-231 cells were maintained in normoglycemic (5 mM glucose) DMEM with 10% FBS supplemented with 100 U/ml penicillin and 100 μg/mL streptomycin in a humidified 5% CO_2 incubator. 2×10^4 cells per well were seeded into 96-well plates and preserved for 24 h in the incubator to help cell attachment. Then, the cells were treated with different concentration of free metformin and metformin-loaded PLGA-PEG NPs (0–40 mM). After 24, 48 and 72 h exposure time, MTT assay was performed to assess the cytotoxic effect of free metformin and metformin-loaded PLGA-PEG NPs. The cell culture medium was replaced and treated with 200 μL of MTT solution (2 mg/mL) and incubated for 4 h. The formed formazan crystals were extracted by adding 200 μL of pure DMSO and incubated for additional 20 min. The absorbance was record at 570 nm using an EL × 800 microplate absorbance reader (Bio Tek Instruments, Winooski, VT) with a reference wavelength of 630 nm. All experiments were repeated 3 times.

2.7. Quantitative real-time PCR assay

T47D and MDA-MB-231 cells were treated with different concentrations of free and drug loaded NPs for 72 h. After the drug exposure time, total RNA was extracted by the Trizol reagent (Invitrogen, Carlsbad, CA) according to the manufacturer's protocol. Purity and quantity of total RNA were verified using NanoDrop ND-1000 spectrophotometer (Thermo Fisher Scientific, Roskilde, Denmark). Additionally, the integrity of RNA samples was assessed using agarose gel electrophoresis on 1.0% agarose gel containing GelRed™ (Biotium, Inc., Hayward, CA, USA). cDNA was synthesized by 2-step RT-PCR kit (Thermo Fisher, K1622) according to the instructions of the manufacturer. Next the level of hTERT gene expression was determined by quantitative real-time PCR technique and Hot Taq EvaGreen qPCR Mix. For real-time PCR, hTERT (Genbank accession: NM_001193376.1) and β-actin primers (Genbank accession: NM-001101) were used. These primers were blasted with primer-blast site on NCBI website. Sequence of forward (F) and reverse (R) primers for hTERT were F: 5′- CCCATTTCATCAGCAAGTTTGG-3′, R: CTTGGCTTTCAGGATGGAGTAG-3′ and primers for β-actin, F: 5′-GGTGAAGGTGACAGCAGT-3′, R: 5′-TGGGGTGGCTTTTAGGAT-3′. The program for real-time PCR reaction contained of an initial denaturation step at 95 °C for 5 min and 38 cycles of denaturation (95 °C for 10 s), annealing (53 °C for 35 s), and extension (72 °C for 20 s). Lastly, amplicons were experienced with melting curve analysis of 65–95 °C. Variations that occurred in telomerase expression amounts between the control and the cells that treated with metformin normalized to β-Actin mRNA amounts, calculated with the $2^{-\Delta\Delta CT}$ method.

2.8. Statistical analysis

All experiments were done in three independent tests. Results were reported as mean ± SD. All statistical analyses were carried out using the software Graph Pad Prism 6.7. Compare data using a tow-way ANOVA was performed. ($p < 0.05$ shows the statistical significance).

3. Results and discussion

3.1. ^{1}HNMR analysis

To confirm the chemical configuration of the PLGA-PEG, ^{1}H NMR spectrum was recorded. ^{1}H NMR spectra confirmed the basic chemical structure of the PLGA-PEG copolymer (Fig. 2). The chemical shifts were determined in ppm by tetramethylsilane (TMS) as an internal control. One of the striking characteristics is a large peak at 3.6 ppm, relating to the methylene groups of the PEG. Results indicated that the PLGA-PEG copolymer was formed successfully.

3.2. Particle size analysis using DLS and FE-SEM

The particle size analysis of PLGA-PEG NPs showed an average size of 210 nm with uniform dispersion of particles also, according to DLS histogram, metformin-loaded PLGA-PEG NPs displayed a

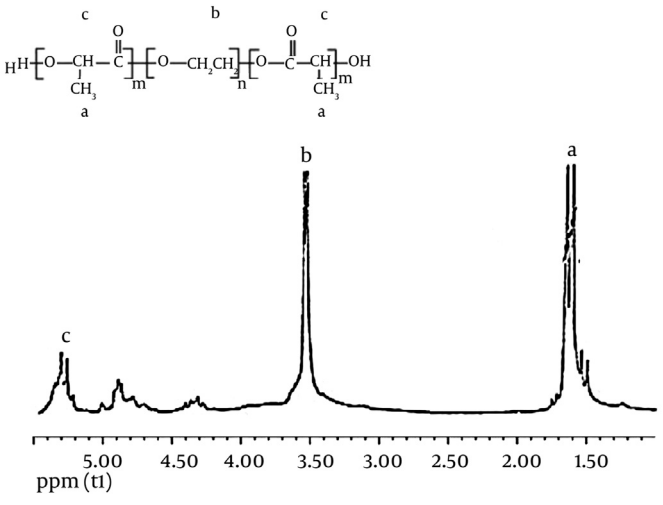

Fig. 2. ^{1}H NMR spectrum of the PLGA-PEG copolymer.

size range of 190–300 nm with an average size of 245 nm (Fig. 3A).

FE-SEM images display that PLGA-PEG and metformin-loaded PLGA-PEG NPs had a smooth surface with uniform and round in shape (Fig. 3B and C). Based on the FE-SEM images, the average size of PLGA-PEG and metformin-loaded PLGA-PEG NPs were around 185 and 220 nm. It is clear that the prepared metformin-loaded PLGA-PEG NPs were larger than blank NPs, indicating that the presence of metformin in the core of the NPs have been increased the volume.

The modest deviation in diameter determined by DLS and FE-SEM is ascribable to changes in the surface states of the samples under the assay conditions applied. Precisely, NPs were in a fully hydrated form when assessed using DLS, while they must be severely dehydrated for SEM characterization. It has been suggested that most cells favorably internalize NPs with a size smaller than 400 nm. So, the size range of the metformin-loaded NPs will be ideal for passive targeting of cancer cells.

3.3. FT-IR analysis

Fig. 4 shows the FTIR results of metformin, where three characteristic bands of metformin were detected between 3372 and 3400, 3296 and 3000-3175 cm^{-1} relative to the NH primary stretching vibration, NH of imines group and NH secondary stretching. Frequently the incidence of this vibration is reduced in the presence of hydrogen bond. The distinctive bands at 1625, 1567-1583 cm^{-1} and a weak peak at 1418 cm^{-1} are assigned to NH primary bending, NH secondary bending and C-N stretching vibrations, respectively. It has been described that C–N stretching of aliphatic amine compounds is commonly weak and appears in the region 1278-1920 cm^{-1}. The peak appeared at 1448-1475 cm^{-1} attributed to C-H bending vibration mode and a weak peak at 2493 cm^{-1} was the characteristic C=N of imines bond. In the case of metformin-loaded PLGA-PEG NPs, all the characteristic bands of metformin and PLGA-PEG was observed. The broad peak at 3300-3600 cm^{-1} was attributed to O-H and N-H bands of polymer and drug. The peak at 2362 cm^{-1} was related to metformin C=N of imines stretching vibration. An intense peak at 1759 cm^{-1} was the characteristic esteric (O-C=O) bands of PLGA section. The peaks at 1508-16369 cm^{-1} are characteristic bands of NH primary bending, NH secondary bending and C-N stretching vibrations of metformin. Other characteristic peaks of PLGA-PEG which indicated C-C, C-O and C-*O*-C were appeared at 1059-1187 cm^{-1}. Therefore, it can conclude the interaction and loading of metformin in PLGA-PEG NPs.

3.4. Entrapment efficiency and in vitro drug release studies

The synthesis yield of PLGA-PEG was calculated to be 94.2%. The encapsulation efficiency (EE) and drug loading efficiency (LE) of metformin-loaded PLGA-PEG NPs was obtained to be ≈ 75% and 5.8%, at higher drug concentrations, the EE and LE was found to be reducing.

In vitro drug release investigations were preformed through the dialysis method at pH 4.4 and 7.4 and the release profile is displayed in Fig. 5. The drug release patterns at pH 7.4 presented a burst release in the first 4 h pursued by a controlled release of metformin during one week and almost 75% of drug was released through 120 h. Absorbed metformin on to the NPs surface and drug encapsulated close to the surface can be the cause for initial burst release, since the degradation rate of the PLGA-PEG close to the surface is high, the quantity of metformin released will be high as well. The cellular uptake of NPs most probably happens through endocytosis or possibly pinocytosis, in which lysosomal processing (pH 4–5) and the further release of metformin may happen at acidic pHs. Thus, it is required to study the release pattern of metformin-loaded NPs in conditions with low pHs. In compared to the release patterns at pH 7.4, the metformin releases at pH 4.4 were considerably quicker in the simulated acidic condition in the lysosome, with near to 80% of the total metformin content being released in the first 48 h.

3.5. Cytotoxicity

MTT assay was applied to assess the cytotoxic effects of different concentrations of free metformin and metformin-loaded PLGA-PEG NPs on T47D and MDA-MB-231 breast cancer cells (Fig. 6).

As expected, both of free and nanoformulated metformin substantially reduced the viability of the both cell lines in time- and dose-dependent manner after 24, 48 and 72 h of treatment and it was found that metformin-loaded PLGA-PEG NPs significantly arrested the growth of the cancer cells than free metformin ($p < 0.05$).

In a similar trend, IC50 values were calculated to quantitate the amount of drug required to kill 50% of cancer cells. The obtained IC50 values for free metformin and metformin-loaded NPs in T47D and MDA-MB-231 were presented in Table 1. Importantly, The IC50s of both free and nanoformulated metformin for MDA-MB-231 cells were lower than T47D cells, indicating enhanced sensitivity of the triple negative phenotype.

MDA-MB-231 cells have aggressive features such as invasion, metastasis and are known to be resistant to numerous anti-cancer

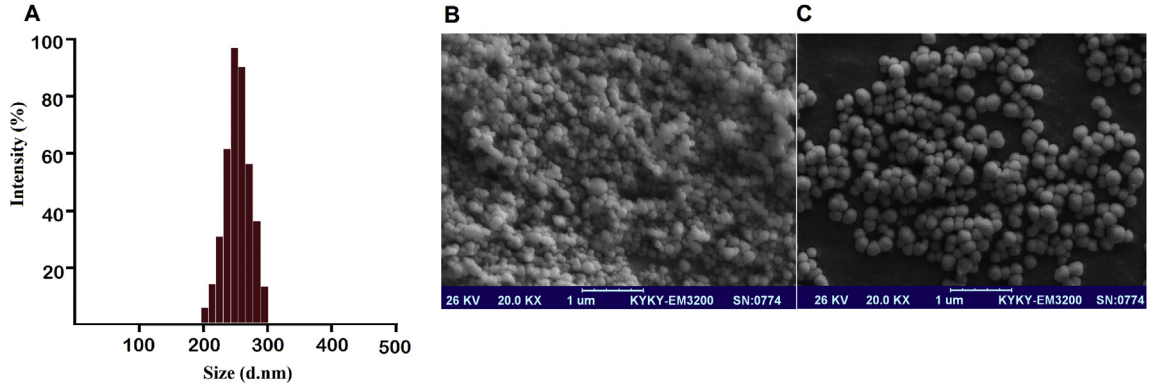

Fig. 3. Dynamic light scattering (DLS) and Field emission scanning electron microscopy (FE-SEM) characterization of NPs. DLS histogram of metformin-loaded NPs (A). FE-SEM images of PLGA-EG NPs (B) and metformin-loaded PLGA-PEG NPs (C).

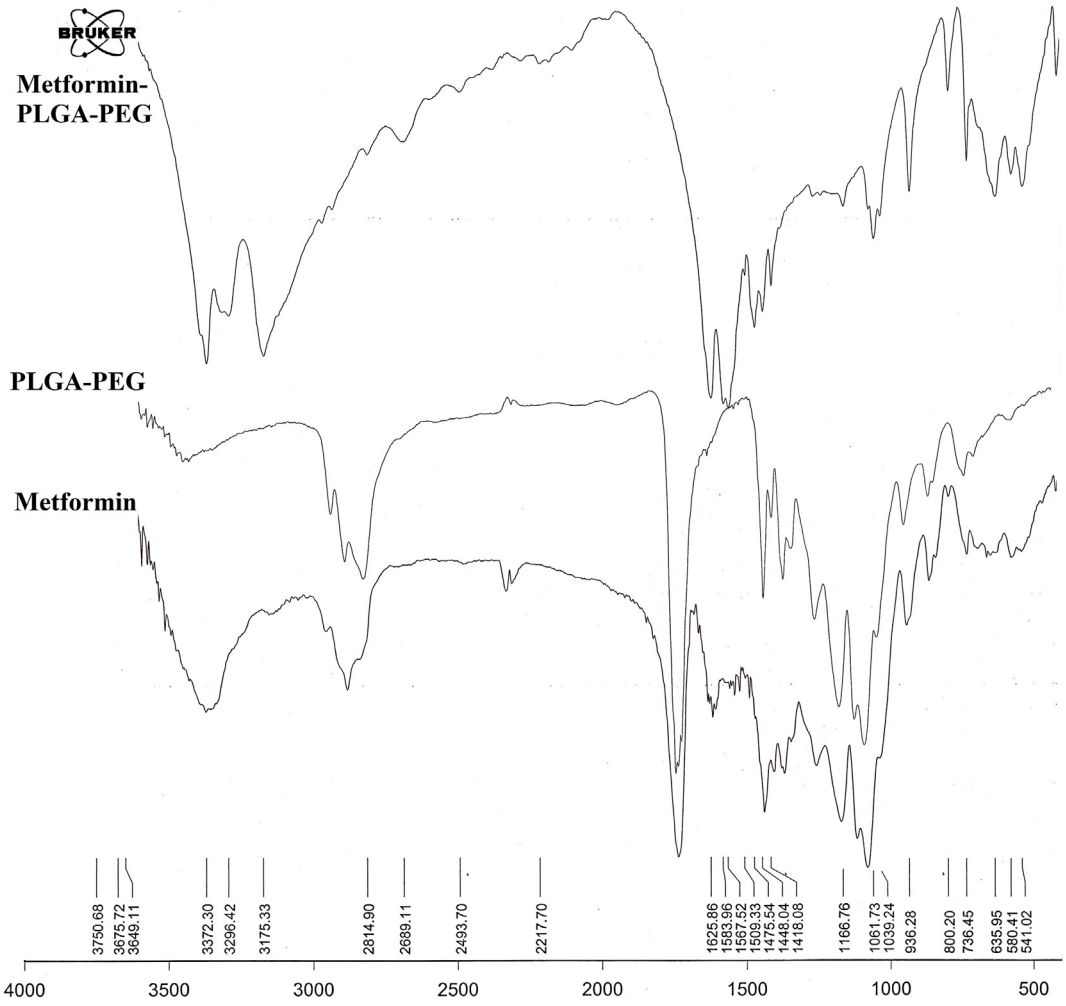

Fig. 4. Infrared spectra of metformin, PLGA-PEG and metformin-loaded PLGA-PEG NPs.

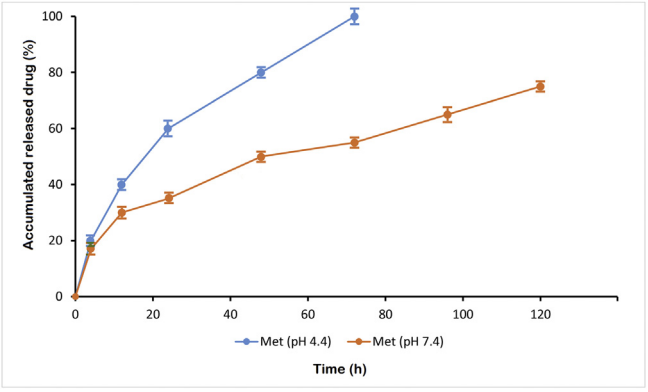

Fig. 5. Drug release profiles of metformin from PLGA-PEG NPs in PBS at pH 4.4 and 7.4. The data are presented as mean ± SD (n = 3).

agents. Besides being triple negative, MDA-MB-231 cells express a mutant p53 and lack the tumor-suppressor kinase LKB1, which make them even more resistant to treatment [21].

LKB1 is a key upstream kinase of the energy sensing enzyme AMPK and the activation of AMPK is the extensively accepted mechanism to clarify the anti-cancer effects of metformin [22,23]. While likely not entirely determined, it is thought that metformin activates AMPK through an LKB1-dependent mechanism, which blocks mTOR, resulting in a strong inhibition of cell growth in numerous cancer cell lines such as non-TN breast cancer cells [24–26]. Consistent with this, it has been proposed that metformin is not capable to prevent the proliferation of MDA-MB-231 cells since these cells do not express LKB1 and therefore metformin fails to stimulate AMPK [24]. However, most of the previous works have evaluated the efficiency of metformin in preventing proliferation of cancer cells via culture conditions that contain high concentrations of glucose [27]. Notably, given the point that metformin-treated breast cancer diabetic cases have improved clinical outcomes in relative to non-metformin treated cases [28], it is possible that normoglycemic conditions may be involved in the level of efficiency of metformin treatment of cancer patients, potentially even in LKB1-deficient cells. Findings of Zordoky and et al. showed that normoglycemia sensitizes the LKB1-deficient triple negative MDA-MB-231 breast cancer cells to the anti-proliferative effect of metformin through an AMPK-dependent mechanism [11]. In accordance with this findings, our results showed that MDA-MB-231 cells were more sensitive to free and nano-encapsulated metformin than T47D cells in normoglycemic conditions.

The enhanced anticancer effect of metformin-loaded NPs was because of the controlled release of the drug and high intracellular concentrations. It is well documented that free therapeutic agents

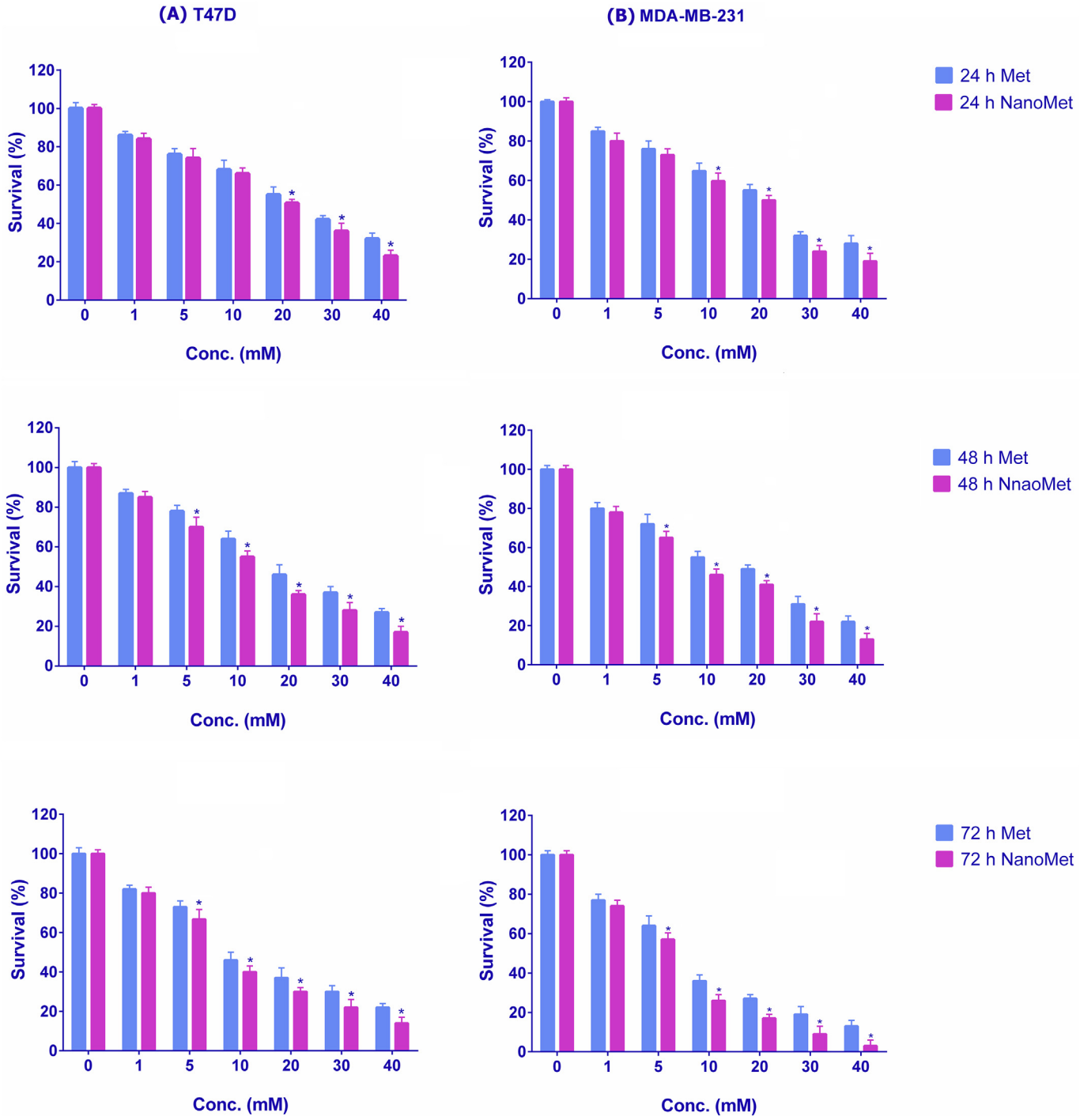

Fig. 6. MTT results of in vitro cytotoxicity of free metformin and metformin-loaded PLGA-PEG NPs against (A) T47D and (B) MDA-MB-231 cells incubated for 24, 48 and 72 h. The data are presented as mean ± SD (n = 3).

Table 1
IC50 values for T47D and MD-MB-231 cells treated with free and nanoformulated metformin after 24, 48 and 72 h drug exposure.

Incubation time (h)	IC_{50} values for T47D		IC_{50} values for MDA-MB-231	
	Free metformin (mM)	Nano metformin (mM)	Free metformin (mM)	Nano metformin (mM)
24	20/86	16/43	17/20	13/19
48	16/68	10/94	12/76	8/28
72	10/36	7/65	6/28	4/34

easily diffuses into the cell membrane while nanoencapsulated drug takes a certain cellular internalization route and releases the drug in a controlled manner [29].

Several groups have attempted to formulate metformin-loaded NPs for its expected application in the treatment of Type 2 diabetes [30–32]. But incorporating nanotechnology for the delivery of metformin into cancer cells, especially in breast cancer, have not yet been fully investigated. In one of the few studies, the ability of Ocarboxymethyl chitosan (O-CMC) NPs as a carrier for metformin against pancreatic cancer cells (MiaPaCa-2) was evaluated [33]. Cytotoxicity findings revealed that the metformin-loaded NPs prompted considerable toxicity on pancreatic cancer cells in relative to L929 normal cells Also, metformin-loaded NPs displayed nonspecific internalization by pancreatic cancer and normal and cells; however, released metformin from the NPs resulted in preferential toxicity on MiaPaCa-2 cells. Following the in vitro results, biological response of the nano-encapsulated metformin has been discovered and its toxicity profile in mice were also documented.

3.6. Expression level of the hTERT

Real-time PCR was performed to quantify hTERT mRNA expression in T47D and MDA-MB-231 cells treated with free and encapsulated forms of metformin in different concentrations after 72 h incubation (Fig. 7). Real-time PCR findings revealed that free and nanoformulated metformin inhibited hTERT gene expression in dose dependent manner in T47D and MDA-MB-231 cells. Furthermore, it was demonstrated that nanoformulated metformin significantly decreased hTERT gene expression compared to free metformin in both cell lines. In comparison between two types of breast cancer cells, it was found that metformin-loaded PLGA-PEG NPs could further decline hTERT expression in MDA-MB-231 cells than T47D cells ($p < 0.05$).

It has been described that metformin can regulate the telomerase activity in cancer cells. In a study by Leigh and colleagues [34], the influence of metformin on cell proliferation and expression of important targets of metformin cell signaling especially hTERT in endometrial cancer cells was evaluated. Findings revealed that metformin strongly inhibit proliferation in a dose dependent manner. Also, metformin caused G1 arrest, reduced hTERT expression and induction of apoptosis. Western immunoblot analysis proved that metformin prompted phosphorylation of AMPK, its immediate downstream mediator, in 24 h of exposure. In parallel, treatment with metformin reduced phosphorylation of S6 protein, a crucial target of the mTOR pathway. Authors concluded that the effect of metformin on hTERT expression may potentially happen as an indirect result of cell cycle arrest instead of a direct effect on hTERT transcription.

4. Conclusion

In this present study, we evaluated the anti-proliferating effect of metformin-loading PLGA-PEG NPs against two types of breast cancer cell lines. Metformin was loaded in PLGA-PEG via double emulsion method (w/o/w) and FT-IR, ^{1}HNMR and FE-SEM analysis verified metformin was successfully loaded on PLGA-PEG. Based on cytotoxicity and hTERT expression analyses, It can be concluded that nano-encapsulation of metformin with PLGA-PEG may be an appropriate and promising strategy for developing effective drug delivery system to clinical application of metformin against breast cancers especially triple negative breast cancers.

Conflict of interest

The authors declare that they have no competing interests.

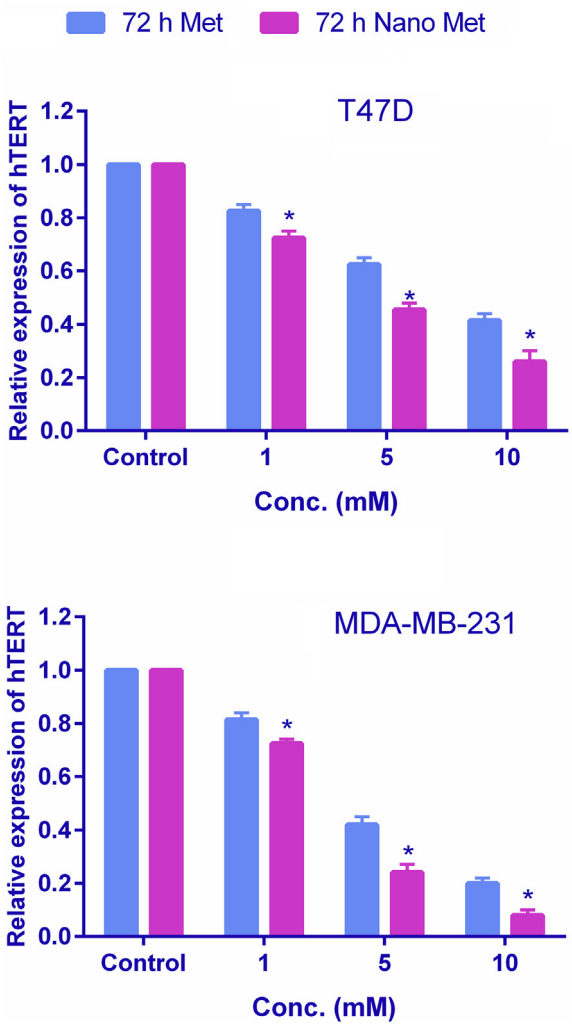

Fig. 7. Level of hTERT mRNA Expression in T47D and MDA-MB-231 cells treated with free metformin and metformin-loaded NPs at different concentrations after 72 h.

Acknowledgments

Authors would like to thank Department of Clinical Biochemistry and Laboratory Sciences, Faculty of Medicine for supporting this project.

References

[1] A. Rami, N. Zarghami, Comparison of inhibitory effect of curcumin nanoparticles and free curcumin in human telomerase reverse transcriptase gene expression in breast cancer, Adv. Pharmceut. Bull. 3 (2013) 127–130.
[2] R.J. Esfahlan, N. Zarghami, A.J. Esfahlan, M. Mollazadeh, K. Nejati, M. Nasiri, The possible impact of obesity on androgen, progesterone and estrogen receptors (ERα and ERβ) gene expression in breast cancer patients, Breast cancer basic Clin. Res. 5 (2011) 227–237.
[3] C.E. DeSantis, S.A. Fedewa, A. Goding Sauer, J.L. Kramer, R.A. Smith, A. Jemal, Breast cancer statistics, 2015: convergence of incidence rates between black and white women, CA A Cancer J. Clin. 66 (2016) 31–42.
[4] J.S. Makki, Telomerase activity in breast cancer, promising marker of disease progression, Telomere Telomerase 2 (2015) 1–5.
[5] M.S. Butler, The role of natural product chemistry in drug discovery, J. Nat. Prod. 67 (2004) 2141–2153.
[6] L. Looi, Telomerase in breast cancer, Malays. J. Pathol. 29 (2007) 47.
[7] L. Wang, J.-C. Soria, B.L. Kemp, D.D. Liu, L. Mao, F.R. Khuri, hTERT expression is a prognostic factor of survival in patients with stage I non-small cell lung cancer, Clin. Canc. Res. 8 (2002) 2883–2889.
[8] V. Shafiei-Irannejad, N. Samadi, B. Yousefi, R. Salehi, K. Velaei, N. Zarghami, Metformin enhances doxorubicin sensitivity via inhibition of doxorubicin

efflux in P-gp-overexpressing MCF-7 cells, Chem. Biol. Drug Des. (2017), http://dx.doi.org/10.1111/cbdd.13078.
[9] R. Farajzadeh, Y. Pilehvar-Soltanahmadi, M. Dadashpour, S. Javidfar, J. Lotfi-Attari, H. Sadeghzadeh, V. Shafiei-Irannejad, N. Zarghami, Nano-encapsulated metformin-curcumin in PLGA/PEG inhibits synergistically growth and hTERT gene expression in human breast cancer cells, Artif. Cells Nanomed. Biotechnol. (2017) 1–9.
[10] B. Liu, Z. Fan, S.M. Edgerton, X.-S. Deng, I.N. Alimova, S.E. Lind, A.D. Thor, Metformin induces unique biological and molecular responses in triple negative breast cancer cells, Cell Cycle 8 (2009) 2031–2040.
[11] B.N. Zordoky, D. Bark, C.L. Soltys, M.M. Sung, J.R. Dyck, The anti-proliferative effect of metformin in triple-negative MDA-MB-231 breast cancer cells is highly dependent on glucose concentration: implications for cancer therapy and prevention, Biochim. Biophys. Acta (BBA)-Gen. Subj. 1840 (2014) 1943–1957.
[12] G.G. Graham, J. Punt, M. Arora, R.O. Day, M.P. Doogue, J. Duong, T.J. Furlong, J.R. Greenfield, L.C. Greenup, C.M. Kirkpatrick, Clinical pharmacokinetics of metformin, Clin. Pharmacokinet. 50 (2011) 81–98.
[13] A. Eatemadi, M. Darabi, L. Afraidooni, N. Zarghami, H. Daraee, L. Eskandari, H. Mellatyar, A. Akbarzadeh, Comparison, synthesis and evaluation of anti-cancer drug-loaded polymeric nanoparticles on breast cancer cell lines, Artif. Cells Nanomed. Biotechnol. 44 (2016) 1008–1017.
[14] P.H. Marathe, Y. Wen, J. Norton, D.S. Greene, R.H. Barbhaiya, I.R. Wilding, Effect of altered gastric emptying and gastrointestinal motility on metformin absorption, Br. J. Clin. Pharmacol. 50 (2000) 325–332.
[15] M. Montazeri, Y. Pilehvar-Soltanahmadi, M. Mohaghegh, A. Panahi, S. Khodi, N. Zarghami, M. Sadeghizadeh, Antiproliferative and apoptotic effect of dendrosomal curcumin nanoformulation in P53 mutant and wide-type cancer cell lines, Anti Canc. Agents Med. Chem. Former. Curr. Med. Chem. Anti Canc. Agents 17 (2017) 662–673.
[16] F. Mohammadian, A. Abhari, H. Dariushnejad, A. Nikanfar, Y. Pilehvar-Soltanahmadi, N. Zarghami, Effects of chrysin-PLGA-PEG nanoparticles on proliferation and gene expression of miRNAs in gastric cancer cell line, Iran. J. Canc. Prev. 9 (2016).
[17] F. Mohammadian, Y. Pilehvar-Soltanahmadi, F. Zarghami, A. Akbarzadeh, N. Zarghami, Upregulation of miR-9 and Let-7a by nanoencapsulated chrysin in gastric cancer cells, Artif. Cells Nanomed. Biotechnol. 45 (2017) 1201–1206.
[18] S. Amirsaadat, Y. Pilehvar-Soltanahmadi, F. Zarghami, S. Alipour, Z. Ebrahimnezhad, N. Zarghami, Silibinin-loaded magnetic nanoparticles inhibit hTERT gene expression and proliferation of lung cancer cells, Artif. Cells Nanomed. Biotechnol. (2017) 1–8.
[19] F. Mohammadian, A. Abhari, H. Dariushnejad, F. Zarghami, A. Nikanfar, Y. Pilehvar-Soltanahmadi, N. Zarghami, Upregulation of Mir-34a in AGS gastric cancer cells by a PLGA-PEG-PLGA chrysin nano formulation, Asian Pac J. Canc. Prev. 16 (2015) 8259–8263.
[20] H. Sadeghzadeh, Y. Pilehvar-Soltanahmadi, A. Akbarzadeh, H. Dariushnejad, F. Sanjarian, N. Zarghami, The effects of nanoencapsulated Curcumin-Fe3O4 on proliferation and hTERT gene expression in lung cancer cells, Anti Canc. Agents Med. Chem. (2017), http://dx.doi.org/10.2174/1871520617666170213115756.
[21] J. Zhou, W. Huang, R. Tao, S. Ibaragi, F. Lan, Y. Ido, X. Wu, Y.O. Alekseyev, M.E. Lendburg, G.-f. Hu, Inactivation of AMPK alters gene expression and promotes growth of prostate cancer cells, Oncogene 28 (2009) 1993–2002.
[22] Z. Shen, X.-F. Wen, F. Lan, Z.-Z. Shen, Z.-M. Shao, The tumor suppressor gene LKB1 is associated with prognosis in human breast carcinoma, Clin. Canc. Res. 8 (2002) 2085–2090.
[23] C. Rosilio, N. Lounnas, M. Nebout, V. Imbert, T. Hagenbeek, H. Spits, V. Asnafi, R. Pontier-Bres, J. Reverso, J.-F. Michiels, The metabolic perturbators metformin, phenformin and AICAR interfere with the growth and survival of murine PTEN-deficient T cell lymphomas and human T-ALL/T-LL cancer cells, Cancer Lett. 336 (2013) 114–126.
[24] R.J. Dowling, M. Zakikhani, I.G. Fantus, M. Pollak, N. Sonenberg, Metformin inhibits mammalian target of rapamycin–dependent translation initiation in breast cancer cells, Canc. Res. 67 (2007) 10804–10812.
[25] Y. Storozhuk, S. Hopmans, T. Sanli, C. Barron, E. Tsiani, J. Cutz, G. Pond, J. Wright, G. Singh, T. Tsakiridis, Metformin inhibits growth and enhances radiation response of non-small cell lung cancer (NSCLC) through ATM and AMPK, Br. J. Canc. 108 (2013) 2021–2032.
[26] B. Li, T. Takeda, K. Tsuiji, A. Kondo, M. Kitamura, T.F. Wong, N. Yaegashi, The antidiabetic drug metformin inhibits uterine leiomyoma cell proliferation via an AMP-activated protein kinase signaling pathway, Gynecol. Endocrinol. 29 (2013) 87–90.
[27] J. Sinnett-Smith, K. Kisfalvi, R. Kui, E. Rozengurt, Metformin inhibition of mTORC1 activation, DNA synthesis and proliferation in pancreatic cancer cells: dependence on glucose concentration and role of AMPK, Biochem. Biophys. Res. Commun. 430 (2013) 352–357.
[28] G. Hou, S. Zhang, X. Zhang, P. Wang, X. Hao, J. Zhang, Clinical pathological characteristics and prognostic analysis of 1,013 breast cancer patients with diabetes, Breast Canc. Res. Treat. 137 (2013) 807–816.
[29] B. Aslan, B. Ozpolat, A.K. Sood, G. Lopez-Berestein, Nanotechnology in cancer therapy, J. Drug Target. 21 (2013) 904–913.
[30] M. Cetin, A. Atila, S. Sahin, I. Vural, Preparation and characterization of metformin hydrochloride loaded-Eudragit® RSPO and Eudragit® RSPO/PLGA nanoparticles, Pharm. Dev. Technol. 18 (2013) 570–576.
[31] N. Sharma, S. Rana, H.G. Shivkumar, R.K. Sharma, Solid lipid nanoparticles as a carrier of matformin for transdermal delivery, Int. J. Drug Deliv. 5 (2013) 137.
[32] U.M.D. Lekshmi, P.N. Reddy, Preliminary toxicological report of metformin hydrochloride loaded polymeric nanoparticles, Toxicol. Int. 19 (2012) 267–272.
[33] K. Snima, R. Jayakumar, A. Unnikrishnan, S.V. Nair, V.-K. Lakshmanan, O-Carboxymethyl chitosan nanoparticles for metformin delivery to pancreatic cancer cells, Carbohydr. Polym. 89 (2012) 1003–1007.
[34] H. Holysz, N. Lipinska, A. Paszel-Jaworska, B. Rubis, Telomerase as a useful target in cancer fighting—the breast cancer case, Tumor Biol. 34 (2013) 1371–1380.